Green Chemistry

PAPER

Direct conversion of methanol to n-C_4H_{10} and H_2 in a dielectric barrier discharge reactor

Received 00th January 20xx,
Accepted 00th January 20xx

DOI: 10.1039/x0xx00000x

www.rsc.org/

L. Wang, [a]† S. Y. Liu, [a]† C. Xu and X. Tu[a, *]

Methanol is an important H-carrier and C1 chemical feedstock. In this paper, the direct conversion of methanol to n-C_4H_{10} and H_2 was achieved for the first time in a dielectric barrier discharge (DBD) non-thermal plasma reactor. The selective formation of n-C_4H_{10} by limiting CO_x (x = 1 and 2) generation was carried out by optimizing different plasma processing parameters including the methanol inlet concentration, discharge power, and pre-heating temperature. The results showed that higher methanol inlet concentration and higher pre-heating temperature favors the formation of n-C_4H_{10}, while higher methanol inlet concentration and lower discharge power can effectively limit the formation of CO. The optimal selectivity for n-C_4H_{10} (37.5%), H_2 (28.9%) and CO (14%) were achieved, with a methanol conversion of 40.0%, at a methanol inlet concentration of 18 mol. %, a discharge power of 30 W and a pre-heating temperature of 140 ^oC using N_2 as a carrier gas. Value-added liquid chemicals (e.g., alcohols, acids, and heavy hydrocarbons) were also obtained from this reaction. Emission spectroscopic diagnostics reveals the formation of various reactive species (e.g., CH, C_2, CN, H and N_2) in the CH_3OH/N_2 DBD. Possible reaction pathways for the formation of n-C_4H_{10} were proposed and discussed.

Introduction

Methanol is an attractive energy-storage carrier, fuel and chemical feedstock and it has gained considerable attention due to the depletion of oil reserves.[1] One of the most important pathways of methanol conversion is to produce hydrogen for fuel cells, since methanol has the advantages of being biodegradable, liquid at room temperature, high in hydrogen content, cheap and abundant (e.g., from biomass, coal, natural gas and syngas).[2] Steam reforming of methanol (reaction R1) and methanol decomposition (reaction R2) have so far been the main routes for methanol conversion into H_2.[3] Considering the supply of hydrogen required for proton exchange membrane fuel cells (PEMFC), hydrogen generated in reaction R2 has to be purified to reach the desired purity by transforming CO into CO_2 through water gas shift reaction (reaction R3), since the Pt-based anode in PEMFC can be easily poisoned when the CO concentration is higher than 10 ppm. Significant efforts have been devoted to catalytic conversion of methanol through the reaction R1, where copper-based and group 8-10 metal-based catalysts have been widely used.[4] The copper-based catalysts have shown high CO_2 selectivity and methanol conversion. However, the long-term stability of these catalysts is poor.[5] Group 8-10 metal-based catalysts have high stability and similar selectivity, but hydrogen production using these catalysts is low compared with that using copper-based catalysts.[4]

$CH_3OH + H_2O \leftrightarrow CO_2 + 3H_2$	$\Delta H^0_{298} = 49.7$ kJ mol^{-1}	R1
$CH_3OH \leftrightarrow CO + 2H_2$	$\Delta H^0_{298} = 90.2$ kJ mol^{-1}	R2
$CO + H_2O \leftrightarrow CO_2 + H_2$	$\Delta H^0_{298} = -41.2$ kJ mol^{-1}	R3

Non-thermal plasma (NTP) technology provides an attractive and promising alternative to the conventional catalysis for the conversion of methanol into value-added fuels and chemicals at low temperatures.[6] In non-thermal plasma, free electrons are highly energetic with a typical electron energy of 1-10 eV, which is sufficient to activate reactant molecules (e.g., methanol) to produce chemically reactive species for the initiation and propagation of chemical reactions according to the radical chain mechanism. It is worth noting that the overall gas temperature of the NTP can be as low as room temperature. Besides, high reaction rate and fast attainment of steady state in the NTP process allows rapid start-up and shutdown of the process compared to thermal and catalytic processes.[7]

Up till now, very limited works have been focused on the use of NTP, either with or without a catalyst for hydrogen production from methanol.[8] Recently, Kim and Lee reported that a methanol conversion of 39.1% can be achieved in a hybrid plasma-catalytic steam reforming of methanol (R1) over

[a] Department of Electrical Engineering and Electronics,
University of Liverpool,
Liverpool L69 3GJ, UK.
E-mail: xin.tu@liverpool.ac.uk
† These authors contributed equally.
* Footnotes relating to the title and/or authors should appear here.
See DOI: 10.1039/x0xx00000x

a $Cu/ZnO/Al_2O_3$ catalyst at 180 ^oC, which is significantly higher than that (5.7%) of the catalytic reforming reaction at the same reaction temperature. These findings suggest that the temperature required for initiating R1 reaction using NTP has been significantly decreased, which is beneficial to prevent the coke formation on the catalyst surface and enhance the stability of the catalyst.[9] Kim and Lee also found that the main role of plasma in generating the synergy effect of plasma and $Cu/ZnO/Al_2O_3$ catalyst is to accelerate the adsorption step of catalytic methanol-steam reforming by pre-activating CH_3OH into numerous reactive species (e.g., CH_3, CH_2OH, and CH_3O).[10] Hueso's group investigated the oxidation of CO produced in a plasma-catalytic decomposition of methanol over a mixture of Cu-Mn oxide catalyst and $BaTiO_3$.[11] The results showed that methanol was almost completely converted into CO and H_2 in the plasma process without a catalyst, whereas the oxidation of CO to CO_2 occurred through the oxygen ions on the surface of the Cu-Mn oxide catalyst when the catalyst was packed in the plasma region. They also mentioned that this oxidation process can be accelerated by adding H_2O in the reaction.

Although the major purpose of methanol conversion is to produce hydrogen, there are other undesired but inevitable products (i.e., CO and CO_2) formed, regardless of which process, e.g., thermal catalysis, plasma process or plasma-catalytic process, was used. Theoretically, a mole of methanol converted forms a mole of CO_x (x = 1 and 2) in the reactions R1 and R2. This means that the carbon atom in a methanol molecule has not been effectively utilized to produce value-added chemicals, but has been consumed to emit greenhouse gas (e.g. CO_2). Actually, density functional theory (DFT) study of methanol conversion via cold plasma performed by Liu's group suggested that it is feasible to synthesize ethylene glycol (EG) directly from methanol, besides CO_x (x = 1 and 2) and H_2, when using a cold plasma.[12] Interestingly, Guo et al recently reported that EG with 71.5% selectivity was experimentally achieved with a methanol conversion of 15.8% in a dielectric barrier discharge plasma using H_2 as a carrier gas.[6] Such a process shows that, by using NTP, the carbon atom of the methanol molecule can take place the carbon coupled reaction to generate value-added chemicals instead of CO and CO_2.

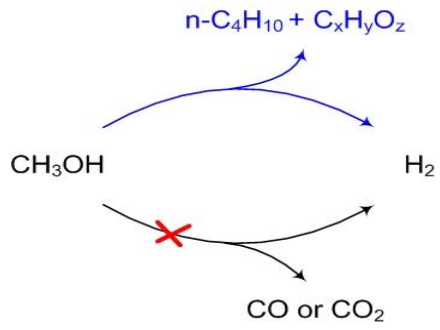

Fig. 1 Schematic representation of methanol conversion using a NTP

In this study, the conversion of methanol into value-added fuels and chemicals (e.g. n-C_4H_{10}) was carried out in a cylindrical dielectric barrier discharge (DBD) reactor using N_2 as a carrier gas. The influence of different plasma processing parameters (e.g. discharge power, methanol inlet concentration and pre-heating temperature) on the plasma conversion of methanol was investigated. This is the first report for direct production of n-C_4H_{10} from methanol using a NTP. The possible reaction pathways for the formation of n-C_4H_{10} in the plasma process were proposed and discussed by combined means of emission spectroscopic diagnostics and the analysis of gas and liquid products.

Experimental

Methanol conversion was carried out in a DBD reactor using N_2 as the carrier gas at atmospheric pressure (Fig. 2). A stainless-steel mesh (ground electrode) was wrapped tightly around the outside of a quartz tube with an external diameter of 22 mm and an inner diameter of 19 mm. The inner high-voltage electrode was a stainless-steel rod with an external diameter of 15 mm, installed along the axis of the quartz tube. The discharge length was about 100 mm with a discharge gap of 2 mm. Methanol was fed into a pre-heating chamber through a syringe pump, and then the vapour of methanol was brought into the DBD reactor using a high-purity nitrogen flow. The flow rate of nitrogen was controlled at 250 ml/min by a mass flow controller. The DBD plasma was connected to an AC power supply with a peak voltage of 30 kV and a variable frequency of 8-12 kHz. The electrical signals were recorded by a four-channel digital oscilloscope (Tektronix, MDO 3024). The discharge power was calculated using Lissajous method.[13] An online power measurement system was used to monitor and control the discharge power of the DBD reactor in real time. The gas temperature in the DBD reactor was measured by a fiber optical temperature probe (OMEGA, FOB102) placed in the plasma discharge. Emission spectra of the CH_3OH/N_2 discharge were recorded by an optical fiber connected to a Princeton Instruments ICCD spectrometer (Model 320 PI, focal length 320 mm) equipped with three gratings (150, 600 and 2400 g/mm gratings).

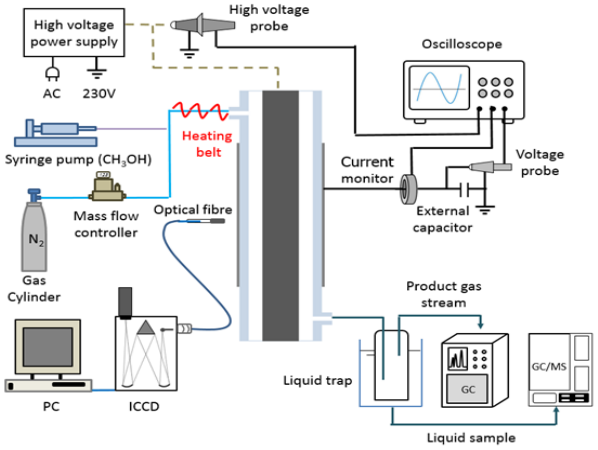

Fig. 2 Schematic diagram of the experimental setup

An ice-water trap was placed at the outlet of the DBD reactor to collect the condensed products. The liquid sample was

analyzed using a gas chromatography-mass spectrometer (GC-MS, Agilent GC 7820A and Agilent MSD 5973). The gaseous products were analyzed using a gas chromatograph (GC) (Shimadzu, GC-2014) equipped with a thermal conductivity detector (TCD) and a flame ionized detector (FID). The GC was calibrated for a wide range of concentrations for each gaseous component using standard gas mixtures (Air Liquid) and other calibrated gas mixtures.

To evaluate the performance of the plasma process, the conversion of methanol is defined as

$$X_{CH_3OH}(\%) = \frac{\text{moles of } CH_3OH \text{ converted}}{\text{moles of initial } CH_3OH} \times 100 \quad (1)$$

The selectivity of the major products can be calculated

$$S_{H_2}(\%) = \frac{\text{moles of } H_2 \text{ produced}}{2 \times \text{moles of } CH_3OH \text{ converted}} \times 100 \quad (2)$$

$$S_{CO}(\%) = \frac{\text{moles of CO produced}}{\text{moles of } CH_3OH \text{ converted}} \times 100 \quad (3)$$

$$S_{C_xH_y}(\%) = \frac{\text{x moles of } C_xH_y \text{ produced}}{\text{moles of } CH_3OH \text{ converted}} \times 100 \quad (4)$$

The energy efficiency of plasma methanol conversion, defined as the moles of methanol converted per kilowatt hour, can be calculated using Eq. (5).

$$\text{Energy Efficiency (mol/kWh)} = \frac{\text{molar conversion rate of } CH_3OH \text{ (mol/min)}}{\text{discharge power (kW)}} \times 60 \quad (5)$$

Results

Effect of methanol inlet concentration on methanol conversion.

Fig. 3 shows the effect of methanol inlet concentration on the conversion of methanol and the energy efficiency of the plasma reaction. Clearly, the conversion of methanol significantly decreased as the methanol concentration increased from 10 to 36 mol.% in the CH_3OH/N_2 mixture. However, the energy efficiency of the plasma process followed the opposite trend. Increasing the methanol concentration significantly enhanced the energy efficiency from 1.8 to 5.0 mol $(kWh)^{-1}$. Fig. 4 shows the distribution of gaseous products as a function of methanol inlet concentration. Three kinds of gaseous products can be identified: H_2, CO_x (i.e., CO and CO_2) and C_xH_y (i.e., CH_4, C_2H_2, C_2H_4, C_3H_8, and n-C_4H_{10}) with H_2, n-C_4H_{10} and CO being the major products. The selectivity of other products was around 1.0%, except C_2H_6 (3.0%) at a methanol inlet concentration of 10 mol. %. Fig. 5 shows that increasing the methanol inlet concentration resulted in a significant decrease of CO selectivity by a factor of 6 (from 21.5 to 3.7%), a decrease of H_2 selectivity from 31.6 to 12.2%, and a slight change of n-C_4H_{10} selectivity. In addition, the formation rate of H_2, n-C_4H_{10} and CO has to be taken into consideration because of the variation of methanol inlet concentration, as shown in Fig. 6. Clearly, the methanol concentration had an inverse influence on the formation rate of n-C_4H_{10} and CO. Increasing the methanol inlet concentration linearly decreases the formation rate of CO but produces more n-C_4H_{10}.

In addition, the liquid products from the reaction were collected by the coolant of ice water and analyzed using GC-MS, as shown in Fig. 7. Results showed that, besides the unconverted methanol, value-added chemicals were also detected in the liquid, such as for the 10 mol. % methanol concentration experiment. These chemicals included alcohols (Ethanol and 1-Propanol, 2-methoxy-), acids (Acetic acid, hydroxyl-), amines (o-Ethylhydroxylamine, Propanamide, 2-hydroxy-, and Methylamine, N, N-dimethyl) and a heavy hydrocarbon (1, 5-heptadien-3-yne). Similar chemicals were also obtained in the produced liquid samples when changing the methanol inlet concentrations. In this work, no gas or liquid phase cyanide products were detected using GC and GCMS. These results also demonstrate that DBD plasma has the potential to transform the carbon atom of methanol molecules to value-added chemicals, not only to CO or CO_2.

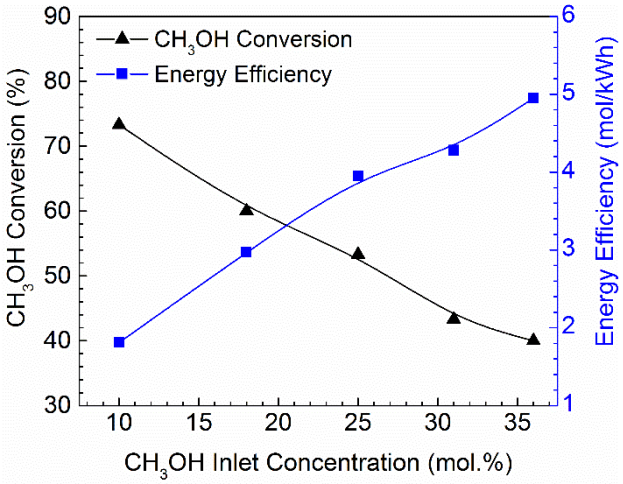

Fig. 3 Methanol conversion and energy efficiency of plasma reaction as a function of methanol inlet concentration (discharge power 30 W, N_2 flow rate 250 ml/min, pre-heating temperature of methanol 80 °C)

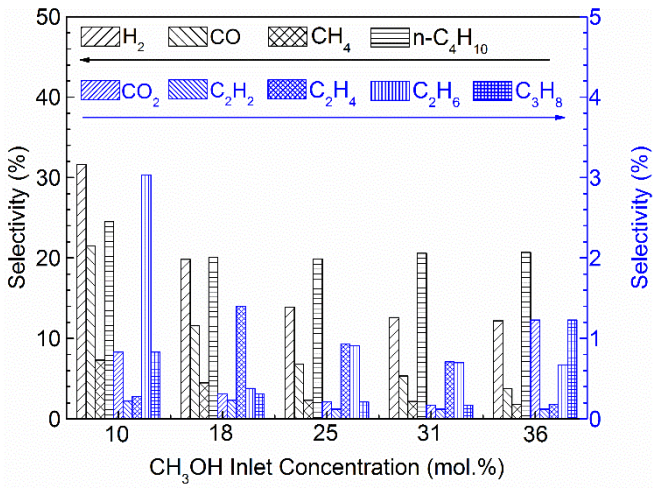

Fig. 4 Effect of methanol inlet concentration on the selectivity of gaseous products (discharge power 30 W, N_2 flow rate 250 ml/min, pre-heating temperature of methanol 80 °C)

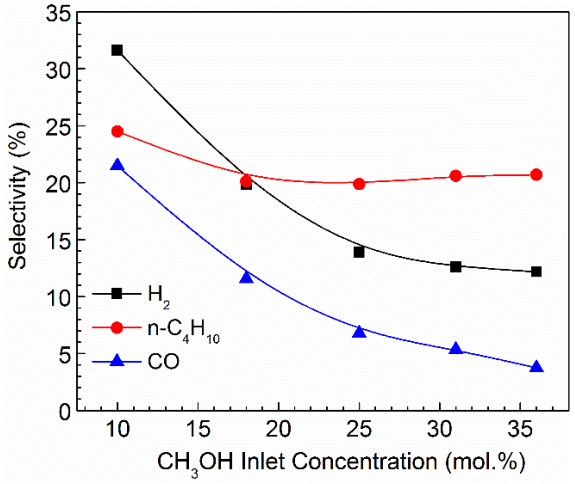

Fig. 5 Selectivity of H_2, CO and n-C_4H_{10} as a function of methanol concentration (discharge power 30 W, N_2 flow rate 250 ml/min, pre-heating temperature of methanol 80 °C)

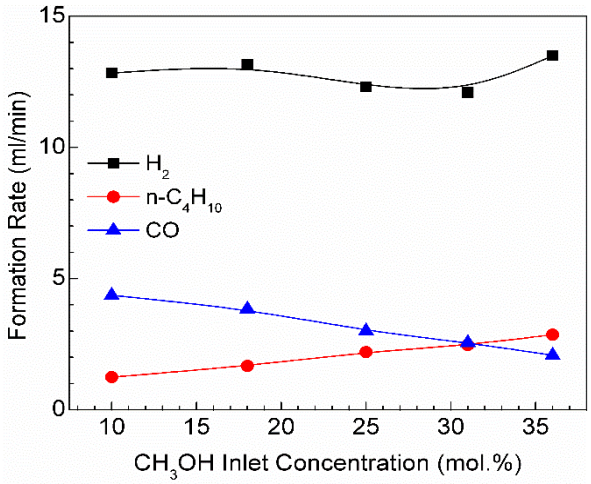

Fig. 6 Formation rate of H_2, CO and n-C_4H_{10} as a function of methanol inlet concentration (discharge power 30 W, N_2 flow rate 250 ml/min, pre-heating temperature of methanol 80 °C)

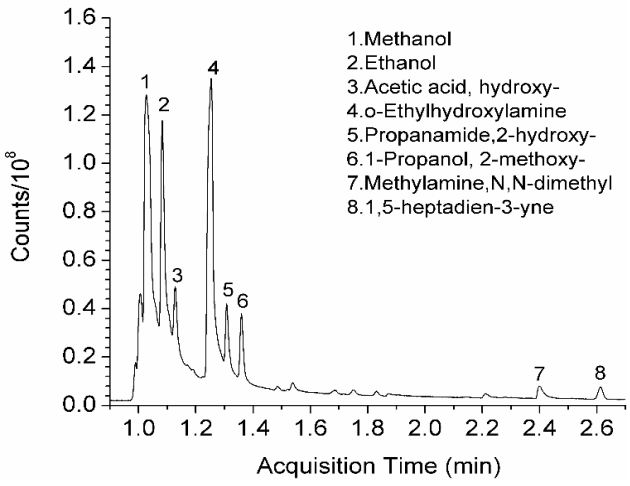

Fig. 7 GC-MS analysis of liquid products collected after plasma conversion of methanol (methanol inlet concentration 10 mol.%, discharge power 30 W, N_2 flow rate 250 ml/min, collection time of liquid sample 0.5 h)

Effect of discharge power on methanol conversion

The influence of discharge power on the reaction performance was evaluated at a methanol concentration of 18 mol. % in CH_3OH/N_2 mixture, as shown in Figs. 8-10. Clearly, increasing the discharge power significantly increased the methanol conversion up to 68.3%. In contrast, the energy efficiency of the plasma process showed the opposite trend, decreasing from 4.2 to 2.0 mol $(kWh)^{-1}$ with the increase of the discharge power from 20 to 50 W (Fig. 8), which was consistent with previous results.[14] Similarly, the major gaseous products were H_2, CO and n-C_4H_{10}, and the selectivity of other products were lower than 1.0% except CH_4 and C_2H_6 which had a selectivity of 2-4% (Fig. 9). Fig. 10 shows that higher discharge power generated more CO and H_2, while the selectivity of n-C_4H_{10} slightly increased with the increase in power. Thus, lowering the discharge power could be an effective way to limit the formation of CO.

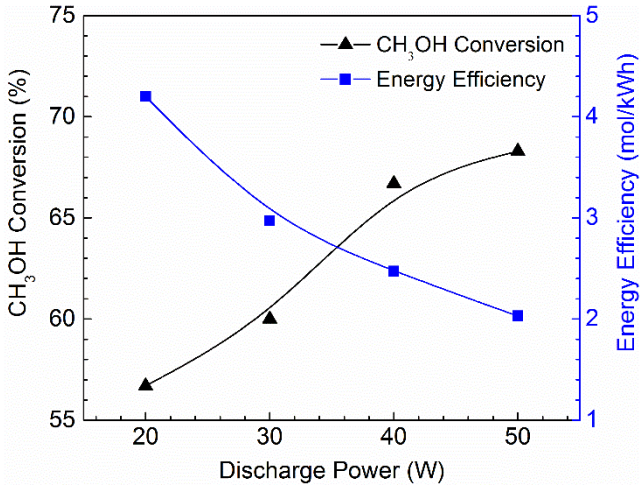

Fig. 8 Methanol conversion and energy efficiency of plasma reaction as a function of discharge power (methanol concentration 18 mol.%, N_2 flow rate 250 ml/min, pre-heating temperature of methanol 80 °C)

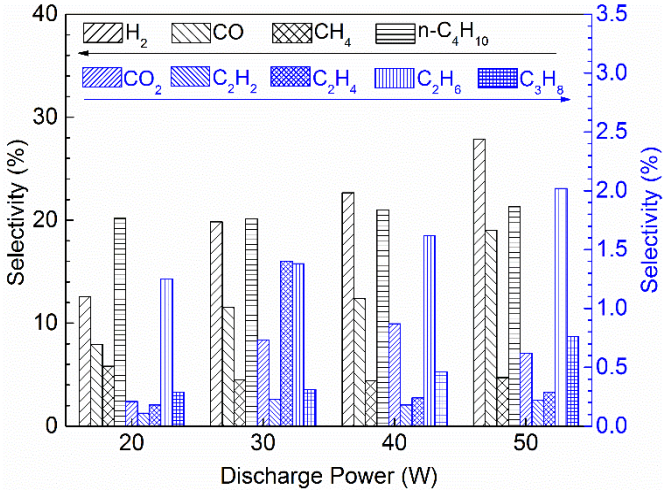

Fig. 9 Effect of discharge power on the distribution of gaseous products (methanol concentration 18 mol.%, N_2 flow rate 250 ml/min, pre-heating temperature of methanol 80 °C).

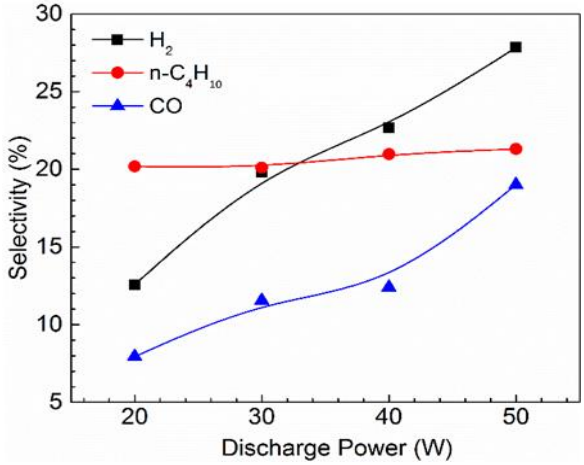

Fig. 10 Selectivity of H_2, CO and n-C_4H_{10} as a function of discharge power (methanol concentration 18 mol.%, N_2 flow rate 250 ml/min, pre-heating temperature of methanol 80 °C).

Effect of pre-heating temperature on methanol conversion

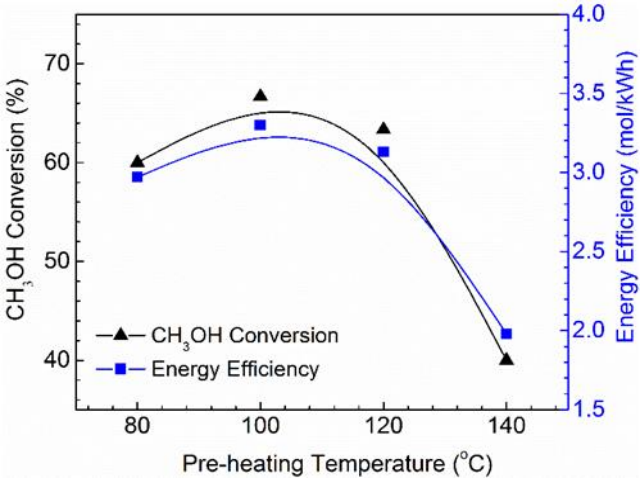

Fig. 11 Methanol conversion and energy efficiency of plasma reaction as a function of pre-heating temperature of methanol (methanol concentration 18 mol.%, discharge power 30 W, N2 flow rate 250 ml/min)

The influence of the pre-heating temperature of methanol on the reaction performance was also examined, as shown in Figs. 11-13. It is interesting to note that the conversion of methanol firstly increased and then decreased with the pre-heating temperature. A maximum methanol conversion of about 67% was achieved at a pre-heating temperature of 100-110 °C (Fig. 11). The energy efficiency of the plasma reaction showed a similar tendency with that of methanol conversion (Fig. 11). H_2, n-C_4H_{10} and CO were still identified as the dominant products (Fig. 12). The pre-heating of methanol increases molecule internal energy and gas temperature in the plasma reaction, which is beneficial to the conversion of methanol. At a discharge power of 30 W, pre-heating methanol to 80 °C increased the gas temperature in the plasma by around 17 °C. Meanwhile the pre-heating of methanol increased the flow rate and decreased the residence time of methanol in the plasma reaction. The combined effects could explain why the conversion of methanol firstly increased and then decreased with the pre-heating temperature. In addition, increasing the pre-heating temperature of methanol enhanced the formation of H_2, n-C_4H_{10} and CO (Fig. 13). In particular, the selectivity of n-C_4H_{10} reached 37.5% at a pre-heating temperature of 140 °C.

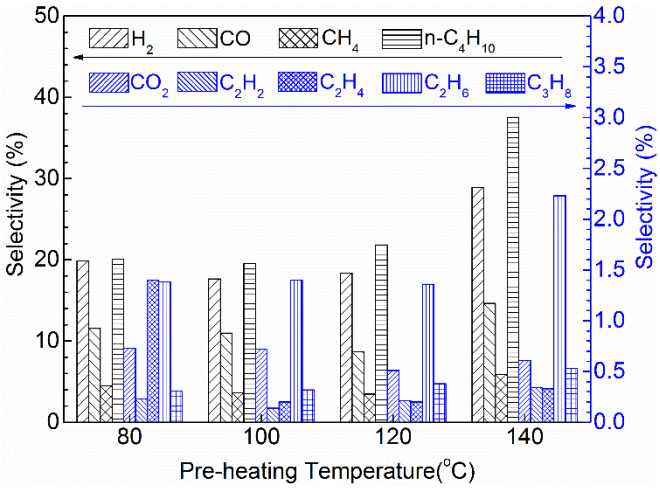

Fig. 12 Effect of pre-heating temperature of methanol on the product distribution of gaseous phase (methanol concentration 18 mol.%, discharge power 30 W, N_2 flow rate 250 ml/min) .

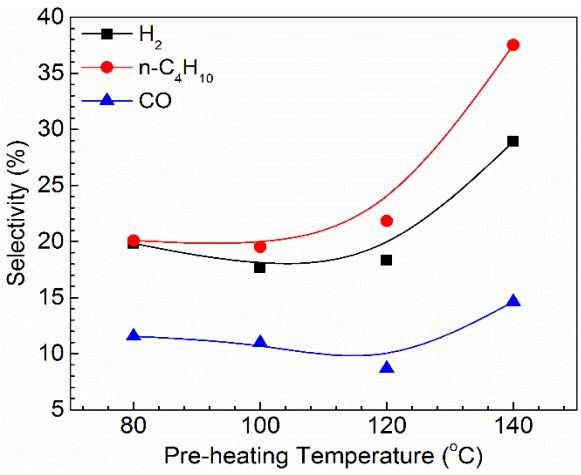

Fig. 13 Selectivity of H_2, CO and n-C_4H_{10} as a function of pre-heating temperature of methanol (methanol concentration 18 mol.%, discharge power 30 W, N_2 flow rate 250 ml/min)

Discussion

Previous studies showed H_2 was the predominant H-containing compound and CO or CO_2 was always the major C-containing product in the plasma conversion of methanol, with or without a catalyst. CH_4, C_2H_2, C_2H_4 and C_2H_6 were reported as minor by-products in this reaction, whereas no other higher hydrocarbons were observed. For example, plasma conversion of methanol was carried out in a direct current rotating gliding arc reactor where H_2 and CO were found as the major products, while only trace amounts of CO_2, CH_4, C_2H_2, C_2H_4 and C_2H_6 were formed with a total selectivity of 0.5-3.8%. No higher hydrocarbons (C > 2) were generated in the gliding arc decomposition of methanol. [15]

Interestingly, in this work, n-C_4H_{10} was identified as the major gaseous hydrocarbon with a selectivity of 20.0-37.5 % in the plasma conversion of methanol. It is noteworthy that increasing the methanol inlet concentration significantly increased the formation of n-C_4H_{10} from 1.2 to 2.9 ml/min (Fig. 6). Correspondingly, the mean electron energy in the plasma gradually decreased with the increase of the methanol inlet concentration, as shown in Fig. 14. These findings suggest that a lower mean electron energy is more favourable to form n-C_4H_{10}.

Previous studies suggested there are seven initial reaction pathways of methanol dissociation by a NTP,[12] as shown in Table 1. In the CH_3OH/N_2 DBD, these intermediate species (e.g., CH_3, CH_2OH, CH_3O, CH_2O, *cis*-HCOH, *trans*-HCOH, and $^1CH_2$ radicals) can be generated by a direct collision of CH_3OH with free electrons, or by a collision of CH_3OH with metastable state molecules such as N_2 ($A^3\Sigma_u^+$).

N_2 ($A^3\Sigma_u^+$), with a rather long radiation lifetime (~2 s) and a high electron energy (~8 eV),[16] plays an important role in the dissociation of CH_3OH into the species listed in Table 1, especially at a lower concentration of CH_3OH. N_2 (B) and N_2 (a') states can also be involved in these reactions instead of the A state.

Among reactions R4-R10, the formation of CH_3 radicals through reaction R4 requires the lowest energy barrier. Besides, DFT study of cold plasma methanol conversion showed that CH_3, CH_2OH and CH_3O radicals in the reactions R4-R6 can be directly generated by inelastic collision of electrons with methanol molecules, whereas the formation of CH_2O, *cis*-HCOH, *trans*-HCOH, and $^1CH_2$ radicals in reactions R7-R10 was a complex process because they had to experience different transition states.[12] The plasma kinetics of electron-molecular reactions also showed the lower threshold energy for reaction R4 (7.94 eV) compared to the reactions R5 (8.28 eV) and R6 (8.88 eV).[17] It means that CH_3 radicals are relatively easy to be formed and the probability of being primary radical is high, followed by CH_2OH and CH_3O.

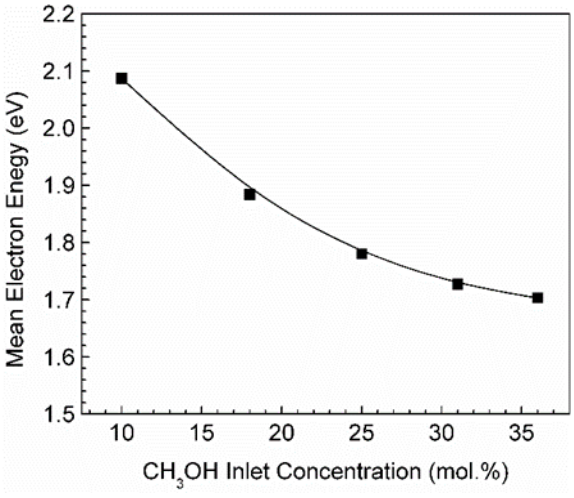

Fig. 14 Mean electron energy of CH_3OH/N_2 plasma as a function of methanol inlet concentration (mean electron energy was calculated using Boltzmann Equation (BE),[18] mean E/n value of ~ 115 Td was used to solve BE cross-section data was from the literature and LXcat.[19])

In this study, a possible reaction pathway of n-C_4H_{10} formation is schematically shown in Fig. 15. Firstly, CH_3 radicals generated through the initial reaction R4 dimerize to form C_2H_6 via neutral-neutral recombination (R11).[20] C_2H_6 can be converted to C_2H_5 by electron impact dissociation (R12)[21] or by H-abstraction reaction (R13)[22]. N_2 excited states can also be involved in the decomposition of C_2H_6. n-C_4H_{10} can be formed from the recombination of two C_2H_5 radicals.[23] Clearly, CH_3 radicals are the initial species for the formation of n-C_4H_{10} in this process. Actually, there is a competitive recombination reaction (R15) to consume CH_3 radicals for CH_4 formation (Fig. 15). Previous study showed that reaction R15 has a similar reaction activate energy (E_a) of 0.5-0.7 kcal and a reaction rate coefficient of about 10^{16} cm^3 (mole s)$^{-1}$ compared to those of R11.[24] However, from the viewpoint of the stability of C_2H_6 and CH_4, C_2H_6 is relatively easy to further convert to other products (e.g, C_2H_2, C_2H_4, C_3H_8, and C_4H_{10}) in plasma, resulting in a decrease in C_2H_6 concentration. The formation of C_2 hydrocarbons can also be confirmed by a weak C_2 swan band in the spectrum of the CH_3OH/N_2 DBD, as presented in Fig. 16. According to the thermal dynamic balance of a chemical reaction, the decrease of C_2H_6 concentration will accelerate the reaction R11 in comparison with reaction R15, which will enhance the formation of n-C_4H_{10}. Such a process agrees with the results achieved in our study. In this experiment, the selectivity of n-C_4H_{10} was always much higher than that of CH_4.

Table 1 Initial reaction channels of methanol dissociation by non-thermal plasma

Reaction		Calculated energy, kcal mol^{-1} (298.15 K)[6, 12]
$CH_3OH \rightarrow CH_3 + OH$	R4	81.51
$CH_3OH \rightarrow CH_2OH + H$	R5	94.57
$CH_3OH \rightarrow CH_3O + H$	R6	100.78
$CH_3OH \rightarrow CH_2O + H_2$	R7	88.62
$CH_3OH \rightarrow$ *cis*-$HCHO + H_2$	R8	85.02
$CH_3OH \rightarrow$ *trans*-$HCHO + H_2$	R9	84.45
$CH_3OH \rightarrow {}^1CH_2 + H_2O$	R10	83.60

According to the radical chain mechanism, the radicals generated in the plasma region can be consumed by recombining with each other to form larger compounds, such as the formation of n-C_4H_{10}, or by further dissociation into smaller fragments. As for CH_3 radicals, in addition to the recombination reaction for the production of n-C_4H_{10} and CH_4 through reactions R11 and R15, they can be dissociated to CH_2 and H by electron impact dissociation (R16) in the plasma region as well. Of course, CH_2 can be further dissociated to CH (Fig. 15) and even to carbon (R17 and R18). The self-recombination of CH_2 and CH radicals leads to the formation of C_2H_4 and C_2H_2 through reactions R19 and R20, respectively. However, the total selectivity of C_2H_2 and C_2H_4 in our experiment was always lower than 2.0%, which indicates that the proportion of CH_3 radical dissociation into CH_2 and CH is much smaller than that of CH_3 radical recombination in our

experiment. This can be confirmed by weak CH bands in the spectrum of the CH_3OH/N_2 DBD (Fig. 16). This is also supported by the results of DFT study,[12] which revealed that the further dissociation of CH_3 radicals required high energy of about 100 kcal/mol (4.2 eV) in reaction R16, about 120 kcal/mol (5.04 eV) in reaction R17 and about 80 kcal/mol (3.36 eV) in reaction R18. In contrast, the energy required in the recombination reactions of radicals is very low and even zero. In addition, the recombination of radicals is an exothermic process, which is relatively favourable in the NTP. Therefore, the reaction R11 is the dominant pathway of CH_3 loss, which leads to the formation of n-C_4H_{10}.

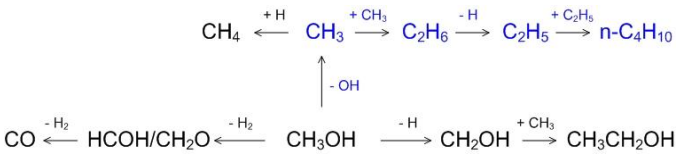

Fig. 15 Possible reaction pathways of n-C_4H_{10}, CH_3CH_2OH and CO formation in CH_3OH/N_2 plasma

$CH_3 + CH_3 \rightarrow C_2H_6$ R11
$C_2H_6 + e \rightarrow C_2H_5 + H + e$ R12
$C_2H_6 + H \rightarrow C_2H_5 + H_2$ R13
$C_2H_5 + C_2H_5 \rightarrow$ n-C_4H_{10} R14
$CH_3 + H \rightarrow CH_4$ R15

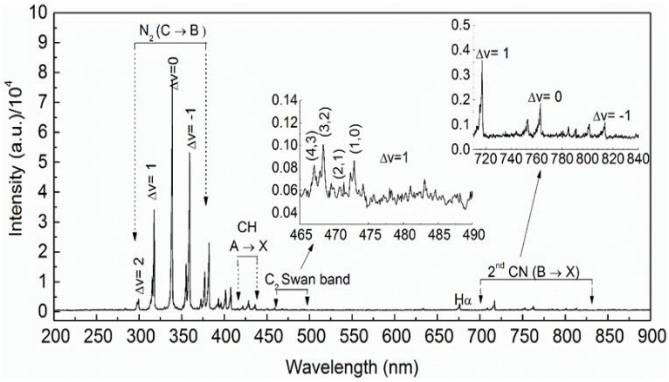

Fig. 16 Optical emission spectroscopy of the CH_3OH/N_2 plasma (methanol concentration 18 mol. %, discharge power 30 W, N_2 flow rate 250 ml/min, 600 g/mm grating, exposure time 0.5 s)

$CH_3 + e \rightarrow CH_2 + H + e$ R16
$CH_2 + e \rightarrow CH + H + e$ R17
$CH + e \rightarrow C + H + e$ R18
$CH_2 + CH_2 \rightarrow C_2H_4$ R19
$CH + CH \rightarrow C_2H_2$ R20

In addition to n-C_4H_{10}, CO is another major gaseous product in our study. It is noteworthy that increasing the methanol concentration significantly decreased the selectivity of CO from 21.5 to 3.7% (Fig. 5), and correspondingly, the formation rate of CO decreased from 4.4 to 2.1 ml/min as well (Fig. 6). In the methanol plasma, the formation of CO was mainly derived from the further dissociation of O-containing species (e.g., CH_2O, *cis*-HCOH and *trans*-HCOH radicals) through reactions R21-R23.[12] In the reactions R4-R10 (Table 1), the formation of O-containing species requires relatively high energy in comparison with that of CH_3 formation. As shown in Fig. 14, the mean electron energy of the CH_3OH/N_2 DBD gradually decreased with the increase of the methanol concentration. Therefore, when the methanol concentration increased, the formation of O-containing species was reduced due to the decrease of mean electron energy in plasma region, which could be the reason why the formation of CO decreased with the increase of methanol concentration. This conclusion can also be evidenced by the effect of discharge power on the CO formation (Fig. 10) which showed that higher discharge power significantly enhanced the formation of CO due to the increase in energy input to the discharge.

$CH_2O + e \rightarrow CO + H_2 + e$ R21
cis-HCOH $+e \rightarrow CO + H_2 + e$ R22
trans-HCOH $+ e \rightarrow CO + H_2 + e$ R23

In addition to the gaseous product, CH_3CH_2OH and o-Ethylhydroxylamine were identified as the major liquid products using GC-MS (Fig. 7). The direct recombination of CH_2OH with CH_3 radical through reaction 24 might be the main reaction pathway for CH_3CH_2OH formation, as shown in Fig 16. The formation of N-containing products (e.g., o-Ethylhydroxylamine) indicates that the carrier gas N_2 participates in the chemical reactions, which can be confirmed by the presence of CN species ($B^2\Sigma \rightarrow X^2\Sigma$, $\Delta v = 1, 0, -1$)[25] in the spectrum of the CH_3OH/N_2 DBD, as shown in Fig. 16.

$CH_2OH + CH_3 \rightarrow CH_3CH_2OH$ R24

Conclusion

In this study, the direct conversion of methanol for the co-production of n-C_4H_{10} and H_2 has been investigated in a DBD reactor using N_2 as the carrier gas. H_2 and n-C_4H_{10} were identified as the major products when varying different plasma process parameters, including the methanol inlet concentration, discharge power and pre-heating temperature of methanol. The selectivity of n-C_4H_{10} significantly increased to 37.5% when increasing the pre-heating temperature of methanol to 140 ^{o}C. Increasing the methanol inlet concentration resulted in a dramatic decrease of CO selectivity from 21.5 to 3.7%, with a slight change of n-C_4H_{10} selectivity, whereas the formation rate of n-C_4H_{10} increased with the increase of methanol inlet concentration. Therefore, higher methanol concentration and higher pre-heating temperature favor the generation of n-C_4H_{10}. The formation of by-product CO in this reaction can be effectively reduced by decreasing the discharge power and increasing methanol inlet concentration. The optimal selectivity for n-C_4H_{10}, H_2 and CO were 37.5%, 28.9 % and 14.0%, respectively, with a methanol

conversion of 40.0% under the reaction conditions of 18 mol. % methanol inlet concentration, 30 W discharge power and 140 ^{o}C pre-heating temperature. In addition, value-added chemicals (e.g., alcohols, acids, and heavy hydrocarbons) were obtained in the reaction. The possible reaction mechanisms have been proposed by means of optical emission spectroscopic diagnostics and the analysis of both gaseous and liquid products. CH_3 radicals have been considered as the initial and key species for the production of n-C_4H_{10}. These results show that non-thermal plasma provides a unique and promising alternative to make full use of methanol to generate value-added chemicals (e.g., n-C_4H_{10}) instead of CO and CO_2 at low temperatures and in an environmentally-friendly way. The selectivity of n-C_4H_{10} and energy efficiency of the plasma process can be further enhanced through the combination of plasma with appropriate catalysts (e.g., SAPO-34 and ZSM-5) together with the optimization of the plasma reactor and operating parameters, which will make this promising green process economically feasible.

Acknowledgements

The support of this work by the UK EPSRC SUPERGEN Hydrogen & Fuel Cell (H2FC) Programme (EP/J016454/1, Ref EACPR_PS5768) is gratefully acknowledged.

Notes and references

1 W. Reschetilowski, *Russ. Chem. Rev.*, 2013, **82**, 624-634; S. N. Khadzhiev, M. V. Magomedova and E. G. Peresypkina, *Petrol. Chem.*, 2014, **54**, 245-269; J. F. Haw, W. Song, D. M. Marcus and J. B. Nicholas, *Accounts Chem. Res.*, 2003, **36**, 317-326.

2 D. R. Palo, R. A. Dagle and J. D. Holladay, *Chem. Rev.*, 2007, **107**, 3992-4021; A. Basile, G. F. Tereschenko, N. V. Orekhova, M. M. Ermilova, F. Gallucci and A. Iulianelli, *Int. J. Hydrogen Energ.*, 2006, **31**, 1615-1622; A. Iulianelli, P. Ribeirinha, A. Mendes and A. Basile, *Renew. Sust. Energ. Rev.*, 2014, **29**, 355-368.

3 Y. Kawamura, N. Ogura and A. Igarashi, *J. Jpn. Petrol. Inst.*, 2013, **56**, 288-297; M. Fan, Y. Xu, J. Sakurai, M. Demura, T. Hirano, Y. Teraoka and A. Yoshigoe, *Int. J. Hydrogen Energ.*, 2015, **40**, 12663-12673; Q. Zhang, G. Liu, L. Wang, X. Zhang and G. Li, *Energ. Fuel*, 2014, **28**, 4431-4439; Y. Xu, J. Yang, M. Demura, T. Hirano, Y. Matsushita, M. Tanaka and Y. Katsuya, *Int. J. Hydrogen Energ.*, 2014, **39**, 13156-13163.

4 S. Sá, H. Silva, L. Brandão, J. M. Sousa and A. Mendes, *Appl. Catal. B: Environ.*, 2010, **99**, 43-57.

5 M. Kurtz, H. Wilmer, T. Genger, O. Hinrichsen and M. Muhler, *Catal. Lett.*, 2003, **86**, 77-80; W. Cao, G. Chen, S. Li and Q. Yuan, *Chem. Eng. J.*, 2006, **119**, 93-98.

6 J. Zhang, Q. Yuan, J. Zhang, T. Li and H. Guo, *Chem. Commun.*, 2013, **49**, 10106-10108.

7 B. Eliasson and U. Kogelschatz, *IEEE T. Plasma. SCI.*, 1992, **19**, 1063-1077; U. Kogelschatz, *Plasma Chem. Plasma P.*, 2003, **23**, 1-46

8 H. Li, J. Zou, Y. Zhang and C. Liu, *Chem. Lett.*, 2004, **33**, 744-745; B. Sarmiento, J. J. Brey, I. G. Viera, A. R. González-Elipe, J. Cotrino and V. J. Rico, *J. Power Sources*, 2007, **169**, 140-143; Y. Wang, Y. You, C. Tsai and L. Wang, *Int. J. Hydrogen Energ.*, 2010, **35**, 9637-9640; H. Zhang, F. Zhu, Z. Bo, K. Cen and X. Li, *Chem. Lett.*, 2015, **44**, 1315-1317; W. Ge, X. Duan, Y. Li and B. Wang, *Plasma Chem. Plasma P.*, 2015, **35**, 187-199; N. Bundaleska, D. Tsyganov, R. Saavedra, E. Tatarova, F. M. Dias and C. M. Ferreira, *Int. J. Hydrogen Energ.*, 2013, **38**, 9145-9157.

9 D. H. Lee and T. Kim, *Int. J. Hydrogen Energ.*, 2013, **38**, 6039-6043.

10 T. Kim, S. Jo, Y. Song and D. H. Lee, *Appl. Energ.*, 2014, **113**, 1692-1699.

11 V. J. Rico, J. L. Hueso, J. Cotrino, V. Gallardo, B. Sarmiento, J. J. Brey and A. R. González-Elipe, *Chem. Commun.*, 2009, 6192-6194.

12 Y. Han, J. Wang, D. Cheng and C. Liu, *Ind. Eng. Chem. Res.*, 2006, **45**, 3460-3467.

13 X. Zhu, X. Gao, C. Zheng, Z. Wang, M. Ni and X. Tu, *RSC Adv.*, 2014, **4**, 37796-37805.

14 D. Mei, X. Zhu, C. Wu, B. Ashford, P. T. Williams and X. Tu, *Appl. Catal. B: Environ.*, 2016, **182**, 525-532.

15 H. Zhang, X. Li, F. Zhu, Z. Bo, K. Cen and X. Tu, *Int. J. Hydrogen Energ.*, 2015, **40**, 15901-15912.

16 C. Kenty, *J. Chem. Phys.*, 1962, **37**, 1567-1568; V. Guerra, P. A. Sá and J. Loureiro, *J. Phys. D: Appl. Phys.*, 2001, **34**, 1754-1755.

17 D. Levko, A. Shchedrin, V. Chernyak, S. Olszewski and O. Nedybaliuk, *J. Phys. D: Appl. Phys.*, 2011, **44**, 145206-145219.

18 G. J. M. Hagellaar and L. C. Pitchford, *Plasma Sources Sci. Technol.*, 2005, **14**,722-733.

19 Morgan database, www.lxcat.net,retrieved on June 12, 2016.

20 D. Walter, and H. H. Grotheer, *Symp. Int. Combust. Proc.*, 1991, **23**, 107-114.

21 S. Jo, D Hoon Lee and Y. Song, *Chem. Eng. Sci.*, 2015, **130**, 101-108.

22 J. R. Cao and M. H. Back, *Int. J. Chem. Kinet.*, 1984, **16**, 961-966.

23 O. Dobis, and S. W. Benson, *J. Am. Chem. Soc.*, 1990, **112**, 1023-1029.

24 N. M. Marinov, W. J.Pitz, C. K. Westbrook, M. J. Castaldi and S. M. Senkan, *Combust. Sci. and Tech.*, 1996, **116-117**, 211-287.

25 H. Zhang, C. Du, A. Wu, Z. Bo, J. Yan and X. Li, *Int. J. Hydrogen Energ.*, 2014, **39**, 12620-12635.